Measurement of the branching ratio $^3H(d,\gamma)/^3H(d,n)$ using thick tritium gas targets

G. L. Morgan, P. W. Lisowski, S. A. Wender, Ronald E. Brown, Nelson Jarmie,
J. F. Wilkerson, and D. M. Drake
Physics Division, Los Alamos National Laboratory, Los Alamos, New Mexico 87545
(Received 9 December 1985)

Measurements have been made of the branching ratio for the reactions $^3H(d,\gamma)^5He/^3H(d,n)^4He$ for several incident deuteron energy ranges between 0 and 0.72 MeV. A stopping length tritium gas target bombarded by a pulsed deuteron beam was used to obtain a high reaction rate as well as provide neutron-gamma ray separation by time of flight. The branching ratio was determined to be $5.6\pm0.6\times10^{-5}$ integrated over the resonance from 0 to 275 keV.

INTRODUCTION

The reaction $^3H(d,\gamma)^5He$ has been studied by a number of workers over the last thirty years. In the earlier work[1-6] most of the emphasis was on the information provided by this reaction on the $A=5$ system. More recently, interest has been focused on this reaction as a possible diagnostic tool for the study of high temperature D-T plasmas.[7-9] The results reported in Refs. 1–6 give values for the $^3H(d,\gamma)/^3H(d,n)$ branching ratio which range from 2×10^{-5} to 3×10^{-4}. A recent report by Cecil and Wilkinson[9] gives a value of $5.4\pm1.3\times10^{-5}$.

Only one[5] of these earlier experiments had the advantage of a tritium gas target. The other investigations were done with tritium absorbed in solid targets with their more difficult background problems. None used the recently developed bismuth germinate (BGO) crystals as gamma-ray detectors. These detectors have a considerably increased γ-ray efficiency over NaI crystals,[10] and for equivalent efficiency a much reduced neutron sensitivity.[11]

In the work reported here a combination of gas target, BGO detector, and pulsed beam time-of-flight (TOF) techniques were used to study the $^3H(d,\gamma)/^3H(d,n)$ branching ratio for several deuteron energy intervals between 0 and 700 keV. Because a thick target was used, the results reported are cross-section-weighted averages over substantial energy ranges.

EXPERIMENTAL PROCEDURE

A schematic diagram of the experimental arrangement is shown in Fig. 1. Pulsed beams of deuterons from the Los Alamos Vertical Van de Graaff accelerator were incident on a gas target cell. These beam pulses had about 1 ns width with a repetition rate of 1.25 MHz. The gas target cell was 1.0 cm in diameter with a length of 2 cm. The entrance window consisted of a molybdenum foil with a thickness of 5.3 mg/cm^2. The downstream end of the target cell contained a beam stop of gold. The cell could be evacuated and filled with either tritium, ^{3}He, or ^{4}He. A calibrated capacitance manometer was used to monitor the cell pressure.

Neutron production in the gas cell was determined using a calibrated NE-213 scintillation counter located at zero degrees with respect to the incident deuteron beam at a distance of 4.13 m. Pulse shape discrimination techniques were used with this detector to eliminate backgrounds due to gamma rays. Figure 2 illustrates a typical

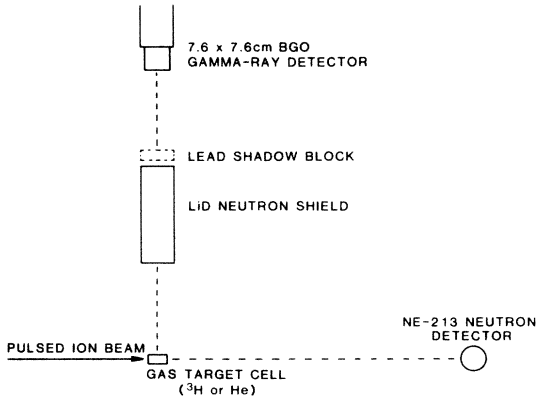

FIG. 1. Schematic diagram of the experimental arrangement.

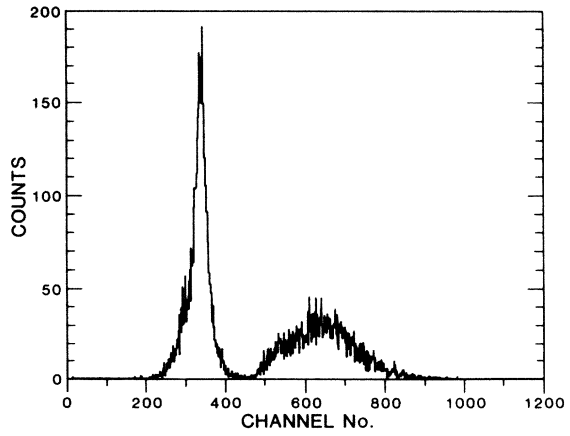

FIG. 2. Pulse-shape discrimination spectrum from a PuBe neutron source placed near the neutron detector. The peak on the left (right) corresponds to γ-ray (neutron) events.

pulse shape spectrum and demonstrates the high quality of separation.

Gamma rays produced in the gas cell were detected with a 7.6 cm diameter by 7.6 cm long BGO scintillation crystal. This detector, located 1.07 m from the target cell and at an angle of 90 deg, had been specially developed[12] to provide fast timing as well as good energy resolution. In order to reduce the neutron fluence incident on the BGO detector, a 25 cm long by 10 cm diameter cylinder of ^{6}LiD was interposed midway between the target cell and BGO. This shadow shield had a transmission of about 0.77 for the 16.7 MeV gamma rays from the ^{3}H(d,γ) reaction, but the uncollided flux of 14 MeV neutrons was reduced by about a factor of 20. A 5.1 cm thick lead shadow shield could also be placed in line between the target and BGO in order to check backgrounds due to gamma rays not coming directly from the target.

The incident deuteron beam was monitored using a current integrator connected to the target cell. A start signal for the TOF measurements was provided by a capacitive pickup loop in the beam line directly in front of the aperture which defined the deuteron beam spot on the gas target entrance window.

Data were recorded for the neutron detector in a TOF spectrum gated by those events which were identified as neutrons using the pulse shape discrimination circuit. Figure 3 shows a TOF spectrum for a deuteron bombarding energy of 0.715 to 0.194 MeV in the gas. For the BGO detector, data were recorded in event mode on magnetic tape in the form of pulse height and TOF parameters. These data could then be sorted off-line. Several pulse height and TOF cuts were displayed on-line to monitor data acquisition.

For each energy region studied, data were taken for several target and shadow bar configurations. In addition to the measurements with tritium in the target, backgrounds were studied by measurements with the lead shadow bar in place to block gamma rays coming directly from the target. Backgrounds associated with the deuteron beam striking the target cell entrance foil and defining apertures were studied by replacing the tritium in the gas

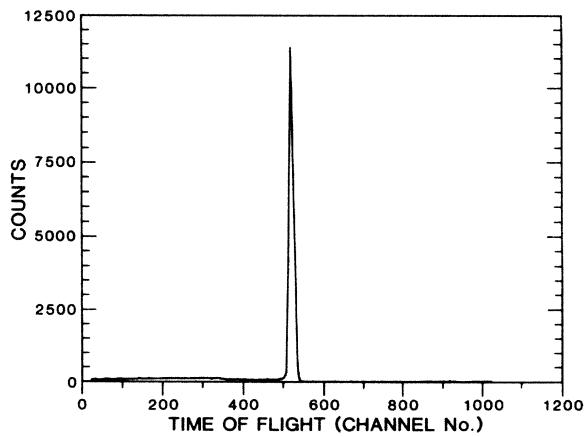

FIG. 3. Time-of-flight spectrum (pulse-shape gated) in the neutron detector for the ^{3}H(d,n) reaction. The peak at about channel 520 is due to 14 MeV neutrons.

TABLE I. Summary of measurements.

Incident deuteron energy (MeV)	Target thickness (mg/cm^2)	Deuteron energy in target (MeV)
1.20	0.344, ^{3}H	0—0.275
1.43	0.344, ^{3}H	0.534—0.715
1.43	0.774, ^{3}H	0.194—0.715
1.43	0.950, ^{3}H	0—0.715
1.43	0.478, ^{3}He	0.236—0.715

cell with an amount of helium gas which gave an equivalent energy loss. Table I summarizes the energy regions studied in the work reported here.

The response of the BGO detector was checked *in situ* by making runs using the ^{3}He(d,γ) reaction for a deuteron energy in the gas of 0.715 to 0.236 MeV. This reaction produced gamma rays of known intensity and an energy essentially the same as that from the ^{3}H(d,γ) reaction (16.7 MeV).

DATA ANALYSIS

For each measurement the neutron production rate from the target cell was determined by integrating the peak in the neutron TOF spectrum and dividing out the detector efficiency and solid angle. The total neutron production rate was obtained by transforming to center-of-mass coordinates and using the fact that the ^{3}H(d,n) reaction is isotropic at these deuteron energies.

For this procedure the weighted average of the laboratory to center-of-mass transformation was calculated in the form

$$G=\int_{E1}^{E2}\frac{g(E)\sigma(E)dE}{S(E)}\Big/\int_{E1}^{E2}\frac{\sigma(E)dE}{S(E)}\ ,$$

where G is the weighted average transformation, $g(E)$ is the transformation at energy E, $\sigma(E)$ is the ^{3}H(d,n) reaction cross section, and $S(E)$ is the stopping power of the tritium gas. $E1$ is the initial deuteron energy in the gas and $E2$ is the lowest energy reached in the gas. A similar procedure was used to calculate the average neutron energy incident on the NE-213 detector for the purpose of determining its efficiency.

As a check on both the calculational procedure and the neutron detector efficiency, the absolute yield from the target was calculated using the relation

$$Y=n\frac{N}{A}\int_{E1}^{E2}\frac{\sigma(E)dE}{S(E)}\ ,$$

where n is the total number of deuterons incident on the target as determined by the current integrator, N is Avogadro's number, and A is the atomic weight of the target. The measured and calculated yields were compared for the measurement with deuteron energies between 0 and 275 keV and found to agree within 1%.

The data from the BGO detector were sorted off-line after the experiment. By summing over all pulse-height values, a TOF spectrum was formed for each run. Figure 4 shows a typical TOF spectrum, in this case for 194—715

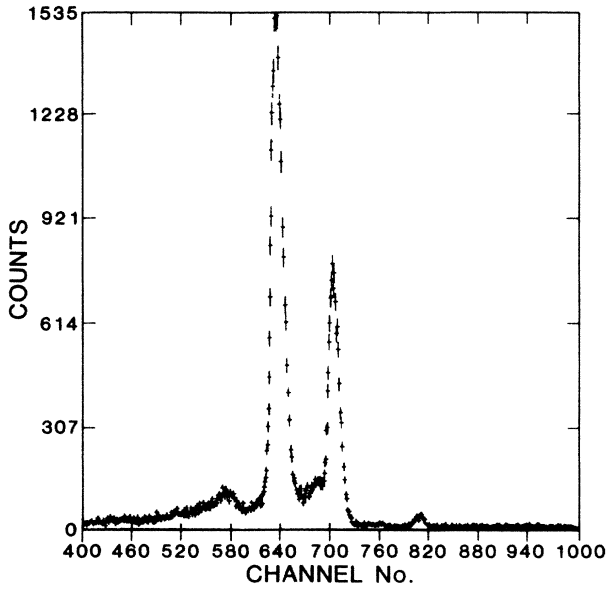

FIG. 4. Time-of-flight spectrum for the BGO detector. The prompt gamma ray is at channel 710. The peak at 640 is due to 14 MeV neutrons.

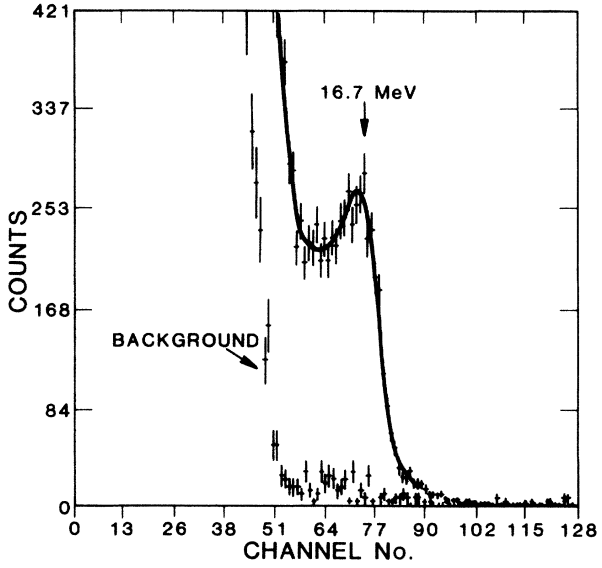

FIG. 5. Pulse height distribution in the BGO detector for those events in the prompt gamma-ray peak of Fig. 4. The background spectrum was obtained with the lead shadow bar in place. The line through the 16.7 MeV gamma-ray pulse height response is a guide to the eye only.

keV deuterons in ^{3}H. This figure demonstrates the effectiveness of the TOF technique in separating those events due to high energy neutrons (the peak near channel 640) from those due to gamma rays from the target (near channel 710). After selecting those time channels corresponding to the prompt gamma ray from the target cell, the data were sorted again to form a pulse-height distribution from events only in these time channels. Figure 5 shows a pulse height spectrum resulting from sorting on the prompt gamma-ray peak in Fig. 4. The points labeled as background are the results of sorting over the same time channels in the data obtained with the lead shadow bar in place.

To determine the gamma-ray yield, the pulse height distribution was summed over channels 60 to 90 (13.5 to 20.1 MeV) in Fig. 5. This was done for the ^{3}H(d,γ) reaction and each of the various background checks. In all cases those backgrounds with the lead shadow bar in place were less than 15% of the foreground values and those backgrounds measured with ^{4}He in the target cell were less than 5%. Corrections were made for the fact that the lead shadow bar transmitted about 4% of the 16.7 MeV gamma rays from the ^{3}H(d,γ) reaction.

The efficiency of the BGO was determined by two independent methods. In the first, the efficiency of the BGO detector was checked from the measurement with ^{3}He in the target cell. The yield of 16.7 MeV gamma rays was calculated using the target thickness, integrated deuteron current, and the cross section data from Ref. 13 in the following equation:

$$Y = n\frac{N}{A}\int_{E1}^{E2}\frac{h(E)dE}{S(E)} ,$$

where A is the atomic weight of ^{3}He, $h(E)$ is the 90° differential cross section for the ^{3}He(d,γ) reaction, and $S(E)$ is the stopping power of the ^{3}He gas. $E1$ and $E2$ are the starting and final energies of the deuterons in the target gas (0.715 and 0.236 MeV). The counts recorded in channels 60 to 90 for this run (after background corrections) are then related to the gamma-ray yield by the equation

$$C = Y\Omega T\epsilon ,$$

where Y is the yield in gamma rays per steradian, Ω is the solid angle subtended by the BGO, T is the transmission of the lithium deuteride shadow shield, and ϵ is the intrinsic efficiency of the BGO crystal for the specified pulse height range. For the purpose of this experiment it is sufficient to determine the product of Ω, T, and ϵ. However, as a check on consistency, ϵ was determined by using a calculated value of T (obtained from the photon cross sections of Ref. 14) and the value of Ω determined from the detector size and distance. The resulting value of the intrinsic efficiency was $\epsilon = 0.394$, which had an uncertainty of about 30% due mostly to the systematic error in the production cross sections of Ref. 13.

In the second method, the efficiency of the detector was calculated using the code CYLTRAN.[15] The result of this calculation was the absolute pulse-height distribution from the detector. This distribution was then integrated over pulse heights from 13.5 to 20.1 MeV to obtain an efficiency corresponding to the region of pulse height utilized for the ^{3}H(d,γ) data. Extensive checks had been made[15] of the accuracy of the CYLTRAN calculations by comparison to absolute efficiency measurements made using a tagged-photon bremsstrahlung source. This work indicated that the calculated efficiencies were accurate to about 10%. The calculated value of the efficiency for 16.7 MeV was 0.447, which agrees within the errors with

TABLE II. Summary of results for the branching ratio $^3H(d,\gamma)/^3H(d,n)$.

Deuteron energy interval (MeV)	Branching ratio ($\times 10^5$)
0.0–0.275	5.6±0.6
0.0–0.715	7.6±0.9
0.194–0.715	7.8±0.9
0.534–0.715	10.6±1.2

the value quoted above from the $^3He(d,\gamma)$ data. For the work reported here the efficiency and its uncertainty were taken from a weighted average of the two determinations.

Using the measured efficiency and the total neutron production data, the background-corrected counts for each measurement were converted to a branching ratio for the reactions $^3H(d,\gamma)/^3H(d,n)$. The overall uncertainty in the result was estimated to be about 11.4%, from the combination of uncertainty in the neutron measurement (5%), BGO efficiency determination (9.5%), and counting statistics in foreground and background (3–4 %).

Implicit in this analysis is the assumption that the channels summed in the pulse height distributions, which included energies from 13.5 to above 16.7 MeV, did not contain any contribution from a possible transition to the first excited state in either ^5He or ^5Li. The present data are obscured by nonsubtracting backgrounds at the lower pulse heights, and no information is available from the present experiment on this question. The existence of this transition for the $^3He(d,\gamma)$ reaction is discussed in Refs. 13, 16, 17, and 18.

RESULTS

The results for the branching ratio $^3H(d,\gamma)/^3He(d,n)$ are summarized in Table II. Figure 6 compares these values with those from previous work. The branching ratio for the deuteron energy interval from 0 to 275 keV is unambiguous since recent results[19] have indicated that in the region of the resonance at 107 keV, the reaction can be described as a single level resonance. This implies that the branching ratio should be independent of deuteron energy. The present measurement agrees well with the value quoted in Ref. 9 for the energy region covering the resonance. At higher deuteron energies there may be contributions from other compound levels as well as direct reaction components. Thus the results for the branching ratios for these energy intervals may be complicated averages involving energy-dependent branching ratios, cross sections, and stopping powers.

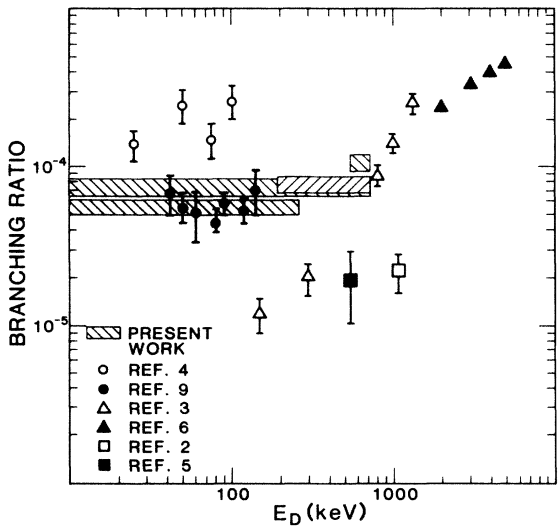

FIG. 6. Comparison of present results for the branching ratio $^3H(d,\gamma)/^3H(d,n)$ with earlier work.

ACKNOWLEDGMENTS

The authors wish to thank J. R. Tesmer and the operations staff of the Los Alamos Ion Beam Facility for their help in this experiment. Thanks are also due to R. V. Poore and J. J. Ross for assistance with the data acquisition computer.

[1]George A. Sawyer and Louis C. Burkhardt, Phys. Rev. **98**, 1305 (1955).
[2]J. Coon and R. Davis, Bull. Am. Phys. Soc. **4**, 365 (1959).
[3]W. Buss, H. Waffler, and B. Ziegler, Phys. Lett. **4**, 198 (1963).
[4]V. M. Bezotosnyi, V. A. Zhmailo, L. M. Surov, and M. S. Shvetsov, Yad. Fiz. **10**, 225 (1969) [Sov. J. Nucl. Phys. **10**, 127 (1970)].
[5]A. Kosiare and H. B. Willard, Phys. Lett. **32B**, 99 (1970).
[6]P. A. Batay-Csorba, Ph.D. thesis, California Institute of Technology, 1975 (unpublished).
[7]S. S. Medley and H. Hendel, Bull. Am. Phys. Soc. **26**, 980 (1982).
[8]F. E. Cecil and David E. Newman, Nucl. Instrum. Methods **221**, 449 (1984).
[9]F. E. Cecil and F. J. Wilkinson III, Phys. Rev. Lett. **53**, 767 (1984).
[10]Darrell M. Drake, Leif R. Nilsson, and John Faucett, Nucl. Instrum. Methods **188**, 313 (1981).
[11]O. Hausser, M. A. Lone, T. K. Alexander, S. A. Kushneriuk, and J. Gascon, Nucl. Instrum. Methods **213**, 301 (1983).
[12]S. A. Wender, G. F. Auchampaugh, and N. W. Hill, Nucl. Instrum. Methods **197**, 591 (1982).
[13]L. Kraus, M. Suffert, and D. Magnac-Valette, Nucl. Phys. **A109**, 593 (1968).
[14]Ellery Storm and Harvey I. Israel, Nucl. Data Tables **A7**, 565 (1970).
[15]S. A. Wender and G. F. Auchampaugh, private communication.
[16]W. Buss, W. Del Bianco, H. Waffler, and B. Ziegler, Nucl. Phys. **A112**, 47 (1968).
[17]H. T. King, W. E. Meyerhof, and R. G. Hirko, Nucl. Phys. **A178**, 337 (1972).
[18]Nelson Jarmie, Ronald E. Brown, F. E. Cecil, D. M. Cole, and R. Philbin, Phys. Rev. C **32**, 690 (1985).
[19]Nelson Jarmie, Ronald E. Brown, and R. A. Hardekopf, Phys. Rev. C **29**, 2031 (1984).